On the Optical Monitoring of Anemia Severity Levels

by

Ankita Dey

A thesis
presented to the University of Waterloo
in fulfillment of the
thesis requirement for the degree of
Master of Mathematics
in
Computer Science

Waterloo, Ontario, Canada, 2015

I hereby declare that I am the sole author of this thesis. This is a true copy of the thesis, including any required final revisions, as accepted by my examiners.

I understand that my thesis may be made electronically available to the public.

Abstract

Anemia is a prevalent medical condition that seriously affects millions of people all over the world. In many regions, not only its initial detection, but also its monitoring are hindered by the limited access to laboratory facilities. This situation has motivated the development of a wide range of optical devices and procedures to assist physicians in these tasks. Although noticeable progress has been achieved in this area, the search for reliable, low-cost and risk-free solutions still continues, and the strengthening of the knowledge base about this disorder and its effects is essential for the success of these initiatives. In this paper, we contribute to these efforts by closely examining the sensitivity of human skin hyperspectral responses (within and outside the visible region of the light spectrum) to reduced hemoglobin concentrations associated with increasing anemia severity levels. This investigation, which involves skin specimens with distinct biophysical and morphological characteristics, is supported by controlled *in silico* experiments performed using a predictive light transport model and measured data reported in the biomedical literature. We also propose a noninvasive procedure to be employed in the monitoring of this condition at the point-of-care.

Acknowledgements

I would like to thank my advisor and supervisor, Dr. Gladimir Baranoski. Without his continued support, motivation and valuable insight, I could never have accomplished this. His dedication to his work and his students as well as his wisdom make him a wonderful supervisor.

I am very grateful to Dr. T. Francis Chen whose technical expertise and valuable advice propelled my research in the right direction.

Last but not the least, my parents and fiance whose love and moral support carried me through the toughest of times.

Dedication

This is dedicated to my mother, for all her strength and persistence.

Table of Contents

List of Tables **vi**

List of Figures **viii**

1 Introduction **1**

2 Methodology **8**
2.1 Simulation Framework Overview 8
2.2 Experimental Sets and Specimen Characterization Data 10
2.3 Sensitivity Measure 19
2.4 Skin Swatches 22

3 *In-Silico* Experiment Results **25**
3.1 Palmar Areas 25
3.2 Nonpalmoplantar Areas 27

4 Monitoring Procedure **35**

5 Conclusion **44**

Bibliography **47**

Index **63**

List of Tables

2.1 HyLIoS parameters employed in the characterization of the skin tissues found in the dorsal surface of the fingers belonging to the two specimens, lightly (LP) and darkly (DP) pigmented, considered in this investigation. 15
2.2 Datasets of specific parameters employed in the characterization the skin tissues found in the palmar fingertip of the two specimens, lightly (LP) and darkly (DP) pigmented, considered in this investigation. 16
2.3 Dataset of general parameters employed in the characterization of the skin tissues found in the dorsal surface and palmar fingertip of the fingers of both specimens considered in this investigation. The refractive indices for the skin layers were measured at 1300 nm as reported in the listed sources. 17
2.4 Anemia severity levels for adult individuals (15 years of age and above). The corresponding reductions in hemoglobin (Hb) concentration considered in this investigation were selected according to values provided in the literature [45, 24, 77]. 18
2.5 Anemia severity levels for children (below 15 years of age) and pregnant women. The corresponding reductions in hemoglobin (Hb) concentration considered in this investigation were selected according to values provided in the literature [45, 24, 77]. 18

4.1 Reflectance values at 570 nm computed for the palmar fingertip of the lightly pigmented (LP) and the darkly pigmented (DP) specimens considering distinct hemoglobin (Hb) concentrations and three angles of incidence, namely 0°, 10° (the default value used in this investigation) and 20°. Each reflectance value was computed using 10^6 sample rays and depicted using a four-digit chopping arithmetic. 42

List of Figures

2.1 Photographs depicting the dorsal and palmar surfaces of the index finger (in a position below heart level) of a lightly pigmented (left) and a darkly (right) pigmented subject. The camera was placed above the specimens and the ambient (non-directional) illumination was provided by fluorescent lamps. . 11

2.2 Absorption spectra of key absorbers found in the skin tissues, namely melanins and functional hemoglobins, whose contents were subjected to variations during this investigation. Top left: extinction coefficient (ε) curves for the melanins [36]. Top right: molar extinction coefficient (ε_m) curves for the functional hemoglobins [57]. Note that the contents of keratin, DNA, uranic acid, beta-carotene, bilirubin, disfunctional hemoglobins lipids and water were also accounted for in this investigation. 14

2.3 Generation of the maximum sensitivity index (MSI) curves for each skin specimen. The input parameters to HyLIoS are specimen parameters (e.g., melanin content, haemoglobin content), measurement parameters (e.g., angle of incidence, wavelength associated with the incident light rays) and biophysical data (e.g., absorption coefficients, refractive indices). HyLIoS then generates a reflectance curve which is used to calculate the sensitivity index across different wavelength ranges, namely, UV, Visible Blue, Visible Green, Visible Red and Infrared regions of the spectrum. 21

2.4 Relative spectral power distributions of three CIE standard illuminants, namely D65, D50 and A, considered in our investigation. While the first two correspond to average daylight with correlated color temperatures of 6504 K and 5503 K respectively, the third one corresponds to a gas-filled tungsten lamp operating at a correlated color temperature of 2856 K [33, 54]. 23
2.5 Diagram depicting the light propagation process leading to the perceived color of human skin. Top: Incident light hits the skin surface and some of it is reflected back which is then perceived by the photoreceptors located in the human eye. Bottom: Skin swatches are obtained from the convolution of the illuminant spectral power distribution ($\phi(\lambda)$) and the reflectance data generated from HyLIoS ($\rho(\lambda)$), which are then transformed into RGB values for display using standard conversion parameters ($\bar{r}, \bar{g}, \bar{b}$)[30] 24

3.1 Modeled skin reflectance curves for the dorsal surface of the fingers of the lightly (top) and the darkly (bottom) pigmented specimen showing the spectral responses elicited by distinct dermal Hb concentrations associated with increasing anemia severity levels, namely baseline (nonanemic level, 147.0 g/L), mild (117.6 g/L), moderate (88.2 g/L) and severe (58.8 g/L). The modeled curves were obtained considering the data provided in Tables 2.1, 2.3 and 2.4. 29
3.2 Mean sensitivity index (MSI) values computed for the modeled anemic skin reflectance curves (mild, moderate and severe) obtained for the dorsal surface of the fingers of the lightly (top) and the darkly (bottom) pigmented specimen (Figure 3.1). The MSI values were computed for each anemic skin reflectance curve (across selected UV (250-400 nm), Visible-B (400-500 nm), Visible-G (500-600 nm), Visible-R (600-700 nm), and NIR (700-850 nm) ranges) with respect to the baseline curve (nonanemic level) associated with the respective specimen. 30

3.3 Skin swatches depicting skin tone variations on the dorsal surface of the fingers of the lightly (top) and the darkly (bottom) pigmented specimens. These variations, which were obtained by reducing the dermal Hb concentration (from left to right, 147.0 g/L, 117.6 g/L, 88.2 g/L and 58.8 g/L), illustrate the visual effects of increasing anemia severity levels, namely baseline (nonanemic level), mild, moderate and severe, respectively (Table 2.4). The swatches were rendered considering a D50 illuminant (Figure 2.4) and using the corresponding skin spectral responses provided by the HyLIoS model (Figure 3.1). 31

3.4 Modeled skin reflectance curves for the palmar fingertips of the lightly (top) and the darkly (bottom) pigmented specimen sshowing the spectral responses elicited by distinct dermal Hb concentrations associated with increasing anemia severity levels, namely baseline (nonanemic level, 147.0 g/L), mild (117.6 g/L), moderate (88.2 g/L) and severe (58.8 g/L). The modeled curves were obtained considering the data provided in Tables 2.2, 2.3 and 2.4. 32

3.5 Mean sensitivity index (MSI) values computed for the modeled anemic skin reflectance curves (mild, moderate and severe) obtained for the palmar fingertips of the lightly (top) and the darkly (bottom) pigmented specimens (Figure 3.4). The MSI values were computed for each anemic skin reflectance curve (across selected UV (250-400 nm), Visible-B (400-500 nm), Visible-G (500-600 nm), Visible-R (600-700 nm), and NIR (700-850 nm) ranges) with respect to the baseline curve (nonanemic level) associated with the respective specimen. 33

3.6 Skin swatches depicting skin tone variations on the palmar fingertips of the lightly (top) and the darkly (bottom) pigmented specimens. These variations, which were obtained by reducing the dermal Hb concentration (from left to right, 147.0 g/L, 117.6 g/L, 88.2 g/L and 58.8 g/L), illustrate the visual effects of increasing anemia severity levels, namely baseline (nonanemic level), mild, moderate and severe, respectively (Table 2.4). The swatches were rendered considering a D50 illuminant (Figure 2.4) and using the corresponding skin spectral responses provided by the HyLIoS model (Figure 3.4). 34

4.1 Skin swatches illustrating skin tone variations on the fingertip of the lightly pigmented specimen (with a baseline Hb concentration equal to 147.0 g/L) resulting from employing distinct light sources (Figure 2.4), namely D65 (top row), D50 (middle row) and A (bottom row), whose default intensity value (left column) was increased by 15% (middle column) and 30% (right column). The swatches were rendered using skin spectral responses provided by the HyLIoS model [8], which, in turn, were obtained using the data provided in Tables 2.2 and 2.3. 36
4.2 Skin swatches illustrating skin tone variations on the fingertip of the darkly pigmented specimen (with a baseline Hb concentration equal to 147.0 g/L) resulting from employing distinct light sources (Figure 2.4), namely D65 (top row), D50 (middle row) and A (bottom row), whose default intensity value (left column) was increased by 15% (middle column) and 30% (right column). The swatches were rendered using skin spectral responses provided by the HyLIoS model [8], which, in turn, were obtained using the data provided in Tables 2.2 and 2.3. 37

Chapter 1

Introduction

Although recent advances in optical technologies are enabling remarkable improvements in the prevention and timely treatment of a wide range of diseases, there are still many challenges ahead, notably involving primary health care for populations that rely on low-resources diagnosis settings. Among these challenges, one can highlight the development of cost-effective procedures and devices for the screening and monitoring of pervasive medical conditions such as anemia, which can compromise the health of individuals of all ages, races, and ethnicities [77]. According to the World Health Organization (WHO), approximately one quarter of the human population is affected by anemia, and this medical condition represents a public health

problem in both industrialised and non-industrialised countries [49, 20].

Anemia is a blood disorder usually associated with a decrease in the number of red blood cells (RBCs) [69] encapsulating hemoglobin proteins [69]. The two functional forms of the hemoglobin (Hb) proteins, namely oxyhemoglobin (O_2Hb) and deoxyhemoglobin (HHb) [6], correspond to the oxygenated and deoxygenated states of hemoglobin molecules, respectively, which play a pivotal role in the maintenance of an individual's normal physiological status. While a O_2Hb molecule contain iron atoms in a ferrous state that allows them to bind with oxygen, a HHb molecule contains iron atoms in a ferric (oxidized) state that prevents this binding.

There are three main types of this disorder, namely iron-deficiency anemia (IDA), pernicious anemia and hemolytic anemia [77, 69]. These are elicited by different factors that can alter the production of healthy RBCs by the bone marrow. This complex biochemical process requires proteins, iron, vitamin B12, folate and small amounts of other minerals and vitamins. For example, IDA, the most common type of anemia, results from a low supply of iron. According to the WHO, it is one of the main factors contributing to the global burden of diseases [49, 20]. In the case of pernicious anemia, it is primarily caused by an insufficient absorption of vitamin B12. Hemolytic

anemia, on the other hand, may take place when a significant number of RBCs are destroyed and removed from the bloodstream through hemolysis before the normal end of their lifespan, and the bone marrow cannot produce enough new RBCs to replace them. This type of anemia can be acquired or inherited. It is also worth mentioning that there are types of anemia, such as "aplastic anemia", associated with a lower than normal presence of other blood formed elements such as white blood cells and platelets. The study of these types of anemia, however, is beyond the scope of this work.

The investigation presented here focuses on the most common types of anemia, which can seriously impair the blood's capability of transporting oxygen from respiratory organs (lungs) to the rest of the body [48]. This, in turn, not only compromises an individual's overall health, but it may also lead to life-threatening situations [77, 69]. Although the Hb concentration in the blood alone cannot be used to diagnose anemia, it can provide useful information for determining its severity level [77]. Accordingly, several optical devices and image-based procedures have been proposed for the low-cost estimation of Hb concentration. These devices and procedures can be loosely divided into two groups: invasive and noninvasive.

Devices belonging to the invasive group tend to provide more accurate

results since they perform *in vitro* measurements on actual blood samples [60, 13]. However, they may still be subjected to errors during the collection and chemical analysis of the samples [42, 14]. In addition, the extraction of blood samples may bring some discomfort and, like any invasive procedure, can incur additional risks for a patient.

Devices and image-based procedures belonging to the noninvasive group, on the other hand, perform *in vivo* estimations that rely on the spectral responses of human skin to variations in Hb concentration [17, 23, 40, 83, 74]. Hence, their predictive capabilities depend on the correctness of the algorithms employed to derive biophysical parameters from reflectance measurements. Since these algorithms usually involve the inversion of models used to simulate the complex interactions of light with various skin tissues and constituent materials, their estimations may be biased by several factors. These include, for example, inacurracies in the models [7], shortcomings of the formulations used in their inversion [67] and, in the case of image-based procedures, issues related to metamerism, the phenomenon whereby colors of specimens match under specified observation conditions despite differences in the specimens' spectral reflectances [34, 54].

In general, the fidelity of the devices and procedures belonging to ei-

ther group is assessed through statistical analyses of compound estimated data. These analyses, in turn, provide qualitative trends with respect to global data, which may obscure possible quantitative limitations of these devices while handling individual cases [81]. Furthermore, in certain instances (*e.g.*, involving spectrophotometry-based monitoring technology such as pulse oximeters [42]), data is collected and analyzed off-line to determine Hb concentrations using proprietary software tools whose underlying algorithms are normally not disclosed for evaluation purposes.

As outlined above, many relevant alternatives exist to assist the diagnosis of anemia, albeit no single device or procedure is superior in all cases. In order to enhance these technologies and propose new effective solutions for the screening and monitoring of this medical condition, we believe that it is necessary to examine their related theoretical and practical constraints from different perspectives. Accordingly, in this thesis, we aim to contribute to these efforts by investigating these constraints using a bottom-up approach. More specifically, we initially assess the sensitivity of human skin hyperspectral responses to fluctuations in dermal Hb concentration associated with increasing anemia severity levels. These responses are sampled within and outside the visible domain, and at distinct cutaneous sites. We then demon-

strate that, although possible variations on skin appearance attributes (*e.g.*, yellowness) can be interpreted as a sign of anemia onset in some patients [77], such visual inspections can be hindered by several physiological (*e.g.*, skin pigmentation) and technical factors (*e.g.*, spectral power distribution of the illuminants). Alternatively, our findings indicate that it is possible to monitor distinct levels of severity of this medical condition using relatively simple noninvasive spectral measurements that are not masked by these factors.

Computer simulations [73, 67, 8, 50], or *in silico* experiments [71], are routinely being employed to accelerate the different cycles of biomedical research involving optical processes that cannot be fully studied through traditional laboratory procedures due to logistic limitations. Among these limitations, one can highlight the difficulties of performing *in vivo* measurements, notably requiring a wide variety of human tissues which may not be available in the first place, as well as the large number of biophysical variables and measurement parameters that need to be controlled during actual experiments. In order to overcome these limitations, the investigation presented in this thesis is also supported by controlled *in silico* experiments. These are performed using a recently developed hyperspectral light transport model for human skin, henceforth referred to as HyLIoS (*H*yperspectral *L*ight *I*mpingement

on *S*kin) [16].

The remainder of this thesis is organized as follows. In the next chapter, we describe our *in silico* experimental framework, including the biophysical data used to characterize the skin specimens considered in our simulations, and introduce the sensitivity measure employed in this investigation. In Chapter 3, we present our results and discuss their practical implications regarding the noninvasive monitoring of anemia. Finally, in Chapter 4, we close the thesis and outline directions for future research in this area.

Chapter 2

Methodology

In this chapter, we will talk about the model we are using for this study as well as the different parameters we are considering for skin specimens. We will show the methods and procedures we used in order to draw our results.

2.1 Simulation Framework Overview

HyLIoS, capable of predictively simulating both the spectral and spatial distributions of light interacting with the skin tissues, takes into account the detailed layered structure of these tissues and the particle nature of their main light attenuation agents, namely the melanosomes, the organelles encapsulating melanin in an aggregated form [55]. In fact, it employs a first princi-

ples simulation approach that incorporates all main light absorbers (keratin, DNA, uranic acid, melanins, hemoglobins, beta-carotene, bilirubin, lipids and water) and scatterers (cells, collagen fibers, melanosomes and melanosome complexes) acting within the skin tissues in the ultraviolet (250-400 nm), visible (400-700 nm) and near-infrared (700-2500 nm) domains.

Within the HyLIoS algorithmic ray optics formulation, a ray interacting with a given skin specimen can be associated with any selected wavelength within the spectral regions of interest. Hence, HyLIoS can provide reflectance readings with different spectral resolutions. For consistency, however, we considered a spectral resolution of 5 nm in all modeled curves depicted in this work. In terms of illumination and collection geometries, the HyLIoS model can provide bidirectional reflectance quantities by recording the direction of the outgoing rays using a virtual gonioreflectometer [41]. In addition, one can obtain directional-hemispherical reflectance quantities by integrating the outgoing rays with respect to the collection hemisphere using a virtual spectrophotometer [10].

To enable the full reproduction of our investigation results, we made HyLIoS available online [52] via a model distribution system [9] along with the supporting biophysical data (*e.g.*, refractive indices and extinction co-

efficients) used in our *in silico* experiments. This framework enables researchers to specify experimental conditions (*e.g.*, angle of incidence and spectral range) and specimen characterization parameters (*e.g.*, pigments and water content) using a web interface, and receive customized simulation results.

2.2 Experimental Sets and Specimen Characterization Data

Usually the assessment of changes in skin appearance attributes is performed considering nonpalmoplantar areas normally exposed to light such as the face and the back of the hand. However, the noninvasive measurement of blood related properties is usually at hypopigmented sites less affected by the presence of melanin such as the palmar fingertips (Figure 2.1).

Although the reasons for the choice of measurement site may be common knowledge among practitioners in this area, however, to the best of our knowledge, it has not been explicitly stated in the literature. In fact, this has been one of the main catalysts for this investigation.

Accordingly, our investigation involved two sets of *in silico* experiments.

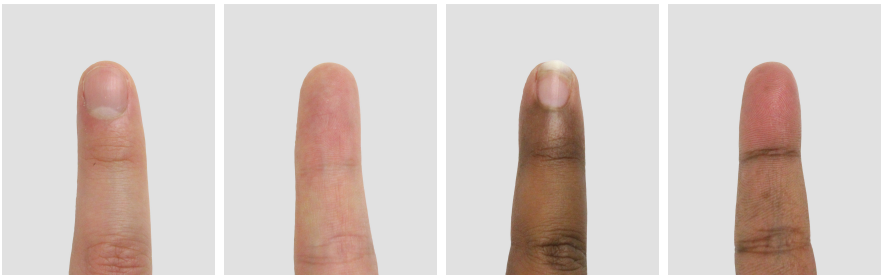

Figure 2.1: Photographs depicting the dorsal and palmar surfaces of the index finger (in a position below heart level) of a lightly pigmented (left) and a darkly (right) pigmented subject. The camera was placed above the specimens and the ambient (non-directional) illumination was provided by fluorescent lamps.

In the first set, we employed HyLIoS to generate directional-hemispherical reflectance curves depicting the spectral effects of reduced Hb concentrations in nonpalmoplantar areas characterized by average pigmentation and morphological parameters such as the dorsal surface of the fingers. In order to expand our scope of observations, these simulations were performed considering skin specimens with different levels of pigmentation, henceforth referred to lightly pigmented (LP) and darkly pigmented (DP). These levels of pigmentation are mostly determined by the presence of the main absorbers acting in the visible domain, namely the melanins (in colloidal and aggregated forms) and the functional hemoglobins, whose absorption spectra is depicted in Figure 2.2. In the second set, we repeat the simulations for the hypopigmented areas, more specifically the palmar fingertips of the LP and DP specimens. In

these simulations, we took into account the particular characteristics of these cutaneous sites, namely the increased epidermal thickness [75], the reduced presence of melanin proteins (more than fivefold lower than in nonpalmoplantar epidermis [78]) and the increased blood fractional volume [18] (especially when the fingertip is in a position below heart level [68]).

Both sets of *in silico* experiments were performed with respect to ultraviolet (UV), visible and near-infraed (NIR) regions of the light spectrum where skin spectral responses to variations on Hb concentration have a higher probability to be detected, more specifically, in the 250-850 nm range [4, 16]. Unless otherwise stated, the resulting reflectance data was obtained considering an angle of incidence of 10°. The specific parameters employed in the characterization of the skin tissues considered in the first and second sets of *in silico* experiments are provided in Tables 2.1 and 2.2, respectively, while characterization parameters employed in both sets of experiments are provided in Table 2.3. In order to account for melanosome degradation in the upper epidermal layers [53], the axes of the melanosomes located in the stratum spinosum and stratum granulosum were set to be, respectively, 50% and 25% of the values considered for the melanosomes in the stratum basale of the LP and and DP specimens depicted in Tables 2.1 and 2.2. We remark that

the values assigned to the specific and general parameters listed in Tables 2.1 to 2.3 were selected based on actual biophysical ranges provided in the scientific literature, and their respective reference sources are also included in these tables. Similarly, the reductions in Hb concentration associated with the anemia severity levels considered in this investigation were also selected according to values provided in the scientific literature as depicted in Tables 2.4 and 2.5.

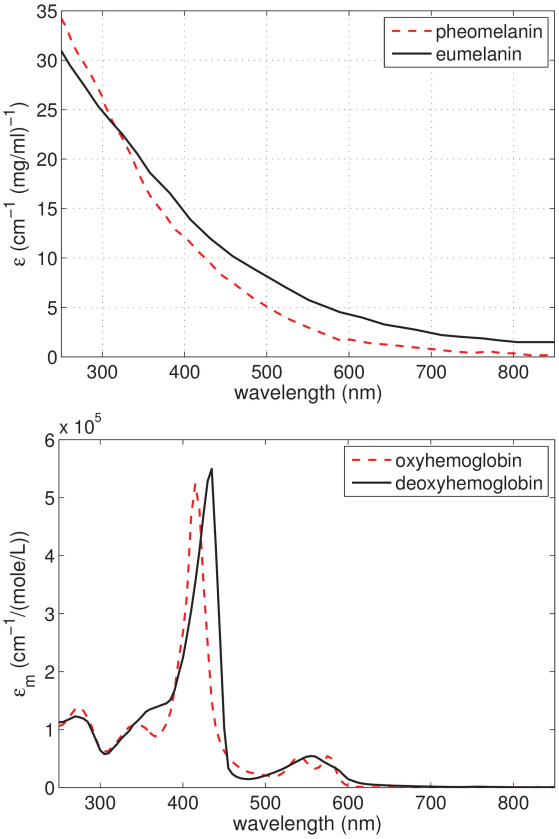

Figure 2.2: Absorption spectra of key absorbers found in the skin tissues, namely melanins and functional hemoglobins, whose contents were subjected to variations during this investigation. Top: extinction coefficient (ε) curves for the melanins [36]. Bottom: molar extinction coefficient (ε_m) curves for the functional hemoglobins [57]. Note that the contents of keratin, DNA, uranic acid, beta-carotene, bilirubin, disfunctional hemoglobins lipids and water were also accounted for in this investigation.

Parameter	LP	DP	Source
Stratum Corneum Thickness (cm)	0.0004	0.0002	[21, 4]
Stratum Granulosum Thickness (cm)	0.0046	0.0015	[75]
Stratum Spinosum Thickness (cm)	0.0046	0.0015	[75]
Stratum Basale Thickness (cm)	0.0046	0.0015	[75]
Papillary Dermis Thickness (cm)	0.02	0.023	[3]
Reticular Dermis Thickness (cm)	0.125	0.2	[3]
Stratum Granulosum Melanosome Content (%)	0.0	5.0	[39, 44]
Stratum Spinosum Melanosome Content (%)	0.0	5.0	[39, 44]
Stratum Basale Melanosome Content (%)	1.0	5.0	[39, 44]
Stratum Granulosum Colloidal Melanin Content (%)	0.9	5.0	[2, 39, 56]
Stratum Spinosum Colloidal Melanin Content (%)	0.9	5.0	[2, 39, 56]
Stratum Basale Colloidal Melanin Content (%)	0.9	5.0	[2, 39, 56]
Stratum Basale Melanosome Dimensions ($\mu m \times \mu m$)	0.41×0.17	0.69×0.28	[55]
Melanosome Eumelanin Concentration (mg/mL)	32.0	50.0	[66, 29]
Melanosome Pheomelanin Concentration (mg/mL)	2.0	4.0	[66, 29]
Papillary Dermis Blood Content (%)	0.5	0.5	[35, 18]
Reticular Dermis Blood Content (%)	0.2	0.2	[35, 18]

Table 2.1: HyLIoS parameters employed in the characterization of the skin tissues found in the dorsal surface of the fingers belonging to the two specimens, lightly (LP) and darkly (DP) pigmented, considered in this investigation.

Parameter	LP	DP	Source
Stratum Corneum Thickness (cm)	0.0004	0.0002	[21, 4]
Stratum Granulosum Thickness (cm)	0.0123	0.006	[75]
Stratum Spinosum Thickness (cm)	0.0123	0.006	[75]
Stratum Basale Thickness (cm)	0.0123	0.006	[75]
Papillary Dermis Thickness (cm)	0.02	0.023	[3]
Reticular Dermis Thickness (cm)	0.125	0.2	[3]
Stratum Granulosum Melanosome Content (%)	0.0	0.25	[78, 39, 44]
Stratum Spinosum Melanosome Content (%)	0.0	0.25	[78, 39, 44]
Stratum Basale Melanosome Content (%)	0.15	0.25	[78, 39, 44]
Stratum Granulosum Colloidal Melanin Content (%)	0.06	0.25	[78, 39, 56]
Stratum Spinosum Colloidal Melanin Content (%)	0.06	0.25	[78, 39, 56]
Stratum Basale Colloidal Melanin Content (%)	0.06	0.25	[78, 39, 56]
Stratum Basale Melanosome Dimensions ($\mu m \times \mu m$)	0.41×0.17	0.69×0.28	[55]
Melanosome Eumelanin Concentration (mg/mL)	32.0	50.0	[66, 29]
Melanosome Pheomelanin Concentration (mg/mL)	2.0	4.0	[66, 29]
Papillary Dermis Blood Content (%)	5.0	5.0	[68, 18, 35]
Reticular Dermis Blood Content (%)	0.5	0.5	[68, 18, 35]

Table 2.2: Datasets of specific parameters employed in the characterization the skin tissues found in the palmar fingertip of the two specimens, lightly (LP) and darkly (DP) pigmented, considered in this investigation.

Parameter	Value	Source
Surface Fold Aspect Ratio	0.1	[64, 47]
Oxygenated Blood Fraction (%)	75.0	[5]
Stratum Corneum Refractive Index	1.55	[65, 22]
Epidermis Refractive Index	1.4	[65, 67]
Papillary Dermis Refractive Index	1.39	[65, 37]
Reticular Dermis Refractive Index	1.41	[65, 37]
Melanin Refractive Index	1.7	[11]
MetHb concentration in Whole Blood (mg/mL)	1.5	[59]
CarboxyHb concentration in Whole Blood (mg/mL)	1.5	[19]
SulfHb concentration in Whole Blood (mg/mL)	0.0	[79]
Whole Blood Bilirubin Concentration (mg/mL)	0.003	[85]
Stratum Corneum Beta-carotene Concentration (mg/mL)	2.1E-4	[43]
Epidermis Beta-carotene Concentration (mg/mL)	2.1E-4	[43]
Blood Beta-carotene Concentration (mg/mL)	7.0E-5	[43]
Stratum Corneum Water Content (%)	35.0	[1, 51]
Epidermis Water Content (%)	60.0	[1, 72]
Papillary Dermis Water Content (%)	75.0	[1, 72]
Reticular Dermis Water Content (%)	75.0	[1, 72]
Stratum Corneum Lipid Content (%)	20.0	[76]
Epidermis Lipid Content (%)	15.1	[62, 15, 1]
Papillary Dermis Lipid Content (%)	17.33	[62, 15, 1]
Reticular Dermis Lipid Content (%)	17.33	[62, 15, 1]
Stratum Corneum Keratin Content (%)	65.0	[26, 61, 27]
Stratum Corneum Urocanic Acid Density (mol/L)	0.01	[82]
Skin DNA Density (mg/mL)	0.185	[70, 1, 25]

Table 2.3: Dataset of general parameters employed in the characterization of the skin tissues found in the dorsal surface and palmar fingertip of the fingers of both specimens considered in this investigation. The refractive indices for the skin layers were measured at 1300 nm as reported in the listed sources.

Severity Level	Hb Reduction (%)	Hb Concentration (g/L)
Baseline	-	147.0.0
Mild	20	117.6
Moderate	40	88.2
Severe	60	58.8

Table 2.4: Anemia severity levels for adult individuals (15 years of age and above). The corresponding reductions in hemoglobin (Hb) concentration considered in this investigation were selected according to values provided in the literature [45, 24, 77].

Severity Level	Hb Reduction (%)	Hb Concentration (g/L)
Baseline	-	125.0
Mild	20	100.0
Moderate	40	75.0
Severe	60	50.0

Table 2.5: Anemia severity levels for children (below 15 years of age) and pregnant women. The corresponding reductions in hemoglobin (Hb) concentration considered in this investigation were selected according to values provided in the literature [45, 24, 77].

2.3 Sensitivity Measure

In order to assess the spectral variation patterns resulting from our *in silico* experiments more systematically, we performed a differential sensitivity analysis [28] on the corresponding modeled reflectance curves across selected spectral ranges (UV (250-400 nm), Visible-B (400-500 nm), Visible-G (500-600 nm), Visible-R (600-700 nm) and NIR (700-850 nm)). This analysis involves the computation of a sensitivity index that provides the ratio of the change in output to the change in a quantity while the other quantities are kept fixed. A ratio equal to 1.0 indicates complete sensitivity (or maximum impact), while a ratio less than 0.01 indicates that the output is insensitive to changes in the selected quantity [30]. Accordingly, we computed the mean sensitivity index (MSI) for the spectral regions of interest to assess the mean ratio of change in reflectance with respect to the change in the selected quantity, namely dermal Hb concentration, associated with the three anemia severity levels (Table 2.4) under study. This index is expressed as

$$MSI = \frac{1}{N}\sum_{i=1}^{N}\frac{|\rho_n(\lambda_i) - \rho_a(\lambda_i)|}{\max\{\rho_n(\lambda_i), \rho_a(\lambda_i)\}}, \tag{2.1}$$

where ρ_n and ρ_a correspond to the reflectances associated with the nonanemic (baseline) and anemic cases, respectively, computed for a given skin specimen, and N is the total number of wavelengths sampled with a 5 nm resolution within a selected spectral region.

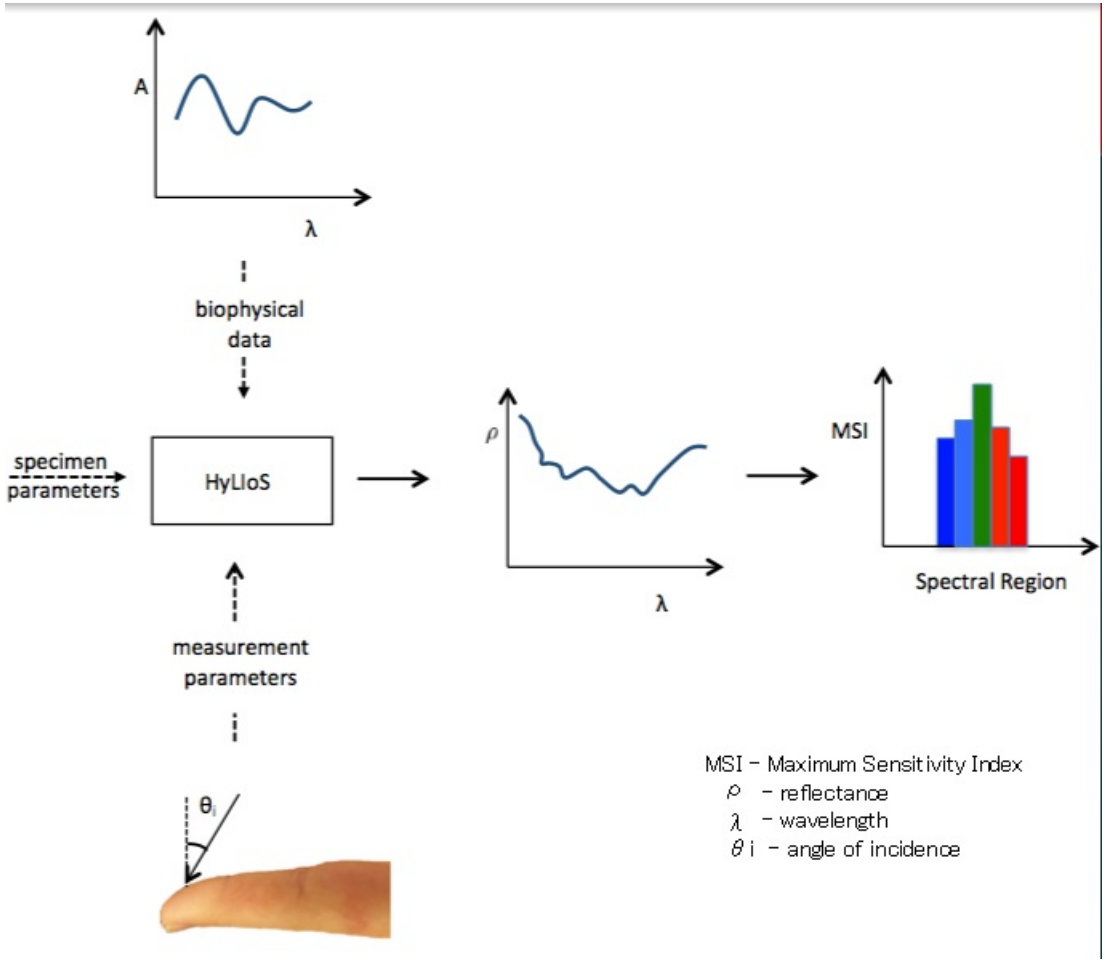

Figure 2.3: Generation of the maximum sensitivity index (MSI) curves for each skin specimen. The input parameters to HyLIoS are specimen parameters (e.g., melanin content, haemoglobin content), measurement parameters (e.g., angle of incidence, wavelength associated with the incident light rays) and biophysical data (e.g., absorption coefficients, refractive indices). HyLIoS then generates a reflectance curve which is used to calculate the sensitivity index across different wavelength ranges, namely, UV, Visible Blue, Visible Green, Visible Red and Infrared regions of the spectrum.

2.4 Skin Swatches

In this investigation, we have also generated skin swatches to demonstrate that the use of visual inspections to detect the onset of anemia and monitor its progression can be hindered by physiological and technical factors. These swatches were rendered using the modeled reflectance data obtained for the LP and DP specimens using HyLIoS, and considering three distinct CIE standard illuminants, whose respective relative spectral power distributions are provided in Figure 2.4. The resulting swatch color is obtained from the convolution of the illuminant spectral power distribution spectrum, the modeled skin reflectance data, and the broad spectral response of the human photoreceptors [31]. This last step was performed employing a standard XYZ to sRGB conversion procedure [7, 63].

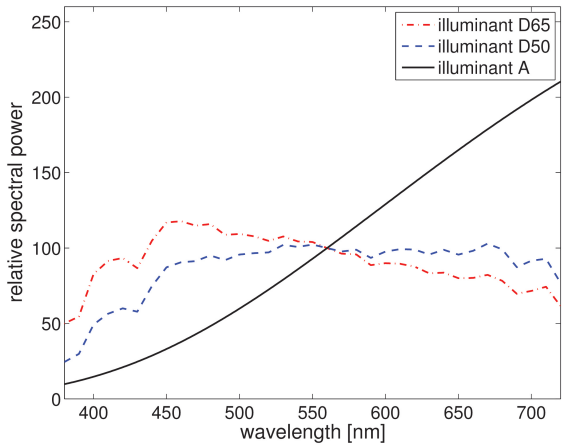

Figure 2.4: Relative spectral power distributions of three CIE standard illuminants, namely D65, D50 and A, considered in our investigation. While the first two correspond to average daylight with correlated color temperatures of 6504 K and 5503 K respectively, the third one corresponds to a gas-filled tungsten lamp operating at a correlated color temperature of 2856 K [33, 54].

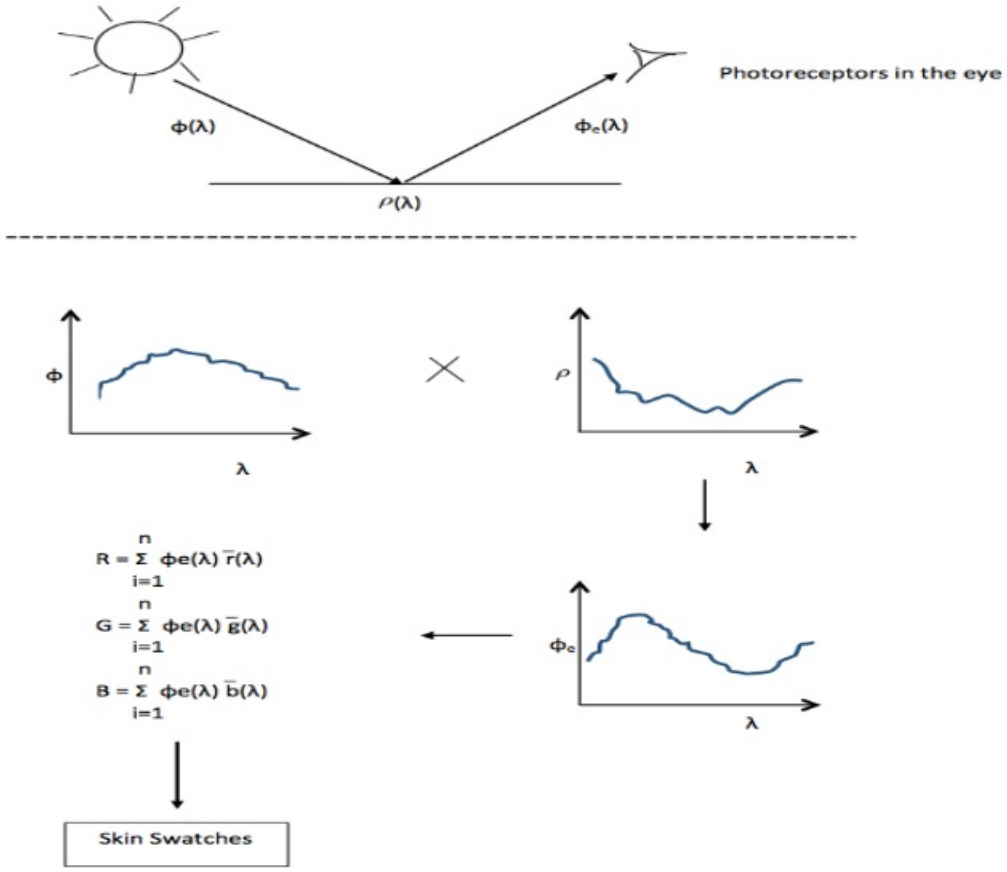

Figure 2.5: Diagram depicting the light propagation process leading to the perceived color of human skin. Top: Incident light hits the skin surface and some of it is reflected back which is then perceived by the photoreceptors located in the human eye. Bottom: Skin swatches are obtained from the convolution of the illuminant spectral power distribution ($\phi(\lambda)$) and the reflectance data generated from HyLIoS ($\rho(\lambda)$), which are then transformed into RGB values for display using standard conversion parameters ($\bar{r}$, $\bar{g}$, $\bar{b}$) [30].

Chapter 3

In-Silico Experiment Results

3.1 Palmar Areas

The results of our first set of *in silico* experiments involving the dorsal surface of the fingers of the LP and DP specimens are presented in Figure 3.1. As expected, these results show that reductions in Hb concentration associated with increasing anemia severity levels have a more noticeable magnifying effect on the reflectance of the LP specimen. This spectral responses less affected by the light attenuation properties of melanin (in colloidal and aggregated forms) than its DP specimen's counterpart.

As indicated by the MSI values presented in Figure 3.2, the impact of

the HB concentration reduction is markedly stronger in the visible region, particularly in the 500-600 nm range, for the LP specimen with respect to three severity levels. This observation can be explained by the fact that, although the UV absorption profile of the hemoglobins (O_2Hb and HHb) are high (Figure 2.2), eumelamin and pheomelanin, albeit in small amounts, have a dominant attenuation role in this spectral region [4, 16]. In the NIR region, on the other hand, not only the hemoglobin absorption profile is relatively low, but light attenuation is also affected by the presence of water and lipids [4, 16].

For the DP specimen, the impact is minor across all selected spectral regions with respect to the mild and moderate levels. It becomes somewhat significant, notably in the visible-G (500-600 nm) range (Figure 3.2), only when the anemia condition reaches the severe level. In this case, the substantial reduction of Hb concentration can slightly counterpose the strong light attenuation performed by the relative large amounts of melanin present in the epidermal tissues. In addition, as further illustrated by the skin swatches depicted in Figure 3.3, while one can notice changes in skin colorimetric parameters, namely lightness and hue (toward a "pale" and a "yellowish" appearance, respectively), following a reduction in Hb concentration in the

LP specimen, such variations, particularly with respect to hue, are not as discernible in the DP specimen.

3.2 Nonpalmoplantar Areas

The results of our second set of *in silico* experiments involving the palmar fingertips of the LP and DP specimens are presented in Figure 3.4. They show that reductions in Hb concentration associated with increasing anemia severity levels have noticeable effects on the spectral responses of both pigmented specimens considered in this investigation. We remark that the palmar fingertips are hypopigmented areas [78] regardless of the native level of pigmentation of an individual (*e.g.*, Figure 2.1), and are characterized by a higher blood volume content in the dermal tissues [18]. Hence, the spectral responses of these cutaneous sites are less affected by the small presence of melanin proteins. Furthermore, as indicated by the MSI values presented in Figure 3.5, the impact of variations in Hb concentration also increases monotonically with the increasing anemia severity levels, and it is markedly stronger in the visible-G (500-600 nm) range for both specimens.

Although the effects resulting from reduced Hb concentrations are clearly

detectable for both specimens through spectrophotometric measurements, the same degree of detection confidence cannot be obtained through the visual inspection of the specimens' skin appearance attributes. More specifically, as illustrated by the skin swatches depicted in Figure 3.6, the same observations reported earlier for the dorsal surface of the finger swatches apply to the palmar fingertip ones, *i.e.*, while we can notice changes in skin lightness and hue following a reduction in Hb concentration in the LP specimen, hue variations, are not as discernible in the DP specimen.

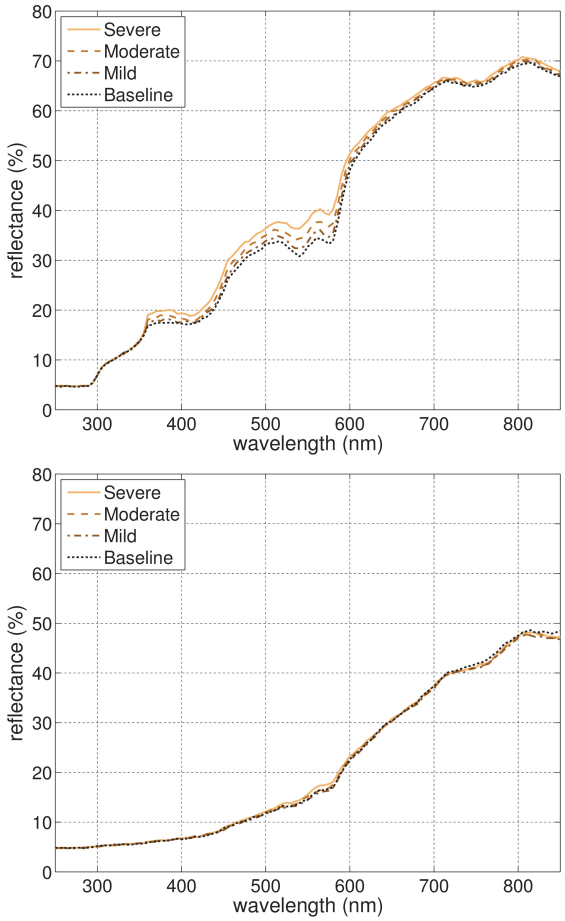

Figure 3.1: Modeled skin reflectance curves for the dorsal surface of the fingers of the lightly (top) and the darkly (bottom) pigmented specimen showing the spectral responses elicited by distinct dermal Hb concentrations associated with increasing anemia severity levels, namely baseline (nonanemic level, 147.0 g/L), mild (117.6 g/L), moderate (88.2 g/L) and severe (58.8 g/L). The modeled curves were obtained considering the data provided in Tables 2.1, 2.3 and 2.4.

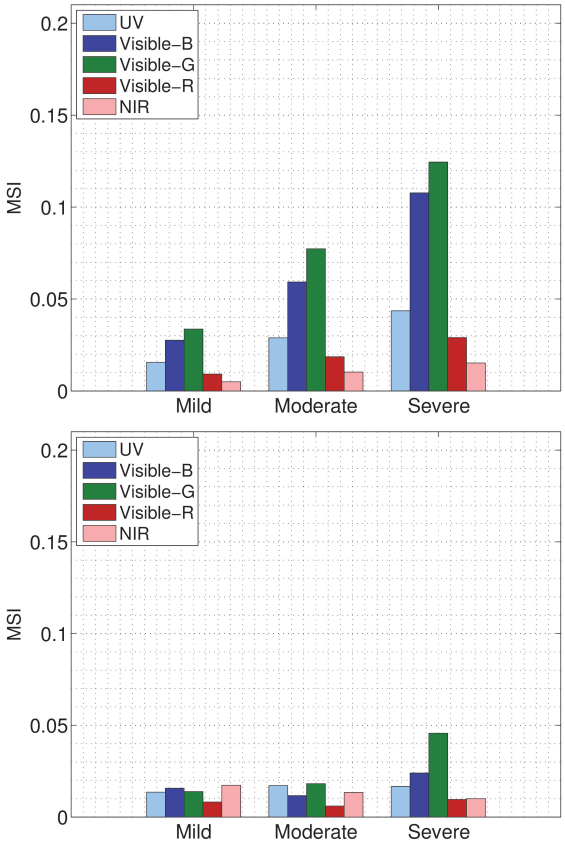

Figure 3.2: Mean sensitivity index (MSI) values computed for the modeled anemic skin reflectance curves (mild, moderate and severe) obtained for the dorsal surface of the fingers of the lightly (top) and the darkly (bottom) pigmented specimen (Figure 3.1). The MSI values were computed for each anemic skin reflectance curve (across selected UV (250-400 nm), Visible-B (400-500 nm), Visible-G (500-600 nm), Visible-R (600-700 nm), and NIR (700-850 nm) ranges) with respect to the baseline curve (nonanemic level) associated with the respective specimen.

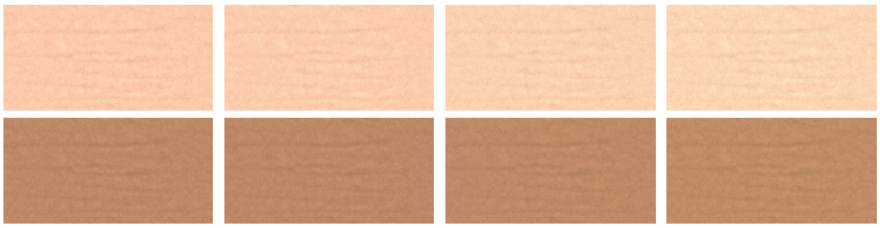

Figure 3.3: Skin swatches depicting skin tone variations on the dorsal surface of the fingers of the lightly (top) and the darkly (bottom) pigmented specimens. These variations, which were obtained by reducing the dermal Hb concentration (from left to right, 147.0 g/L, 117.6 g/L, 88.2 g/L and 58.8 g/L), illustrate the visual effects of increasing anemia severity levels, namely baseline (nonanemic level), mild, moderate and severe, respectively (Table 2.4). The swatches were rendered considering a D50 illuminant (Figure 2.4) and using the corresponding skin spectral responses provided by the HyLIoS model (Figure 3.1).

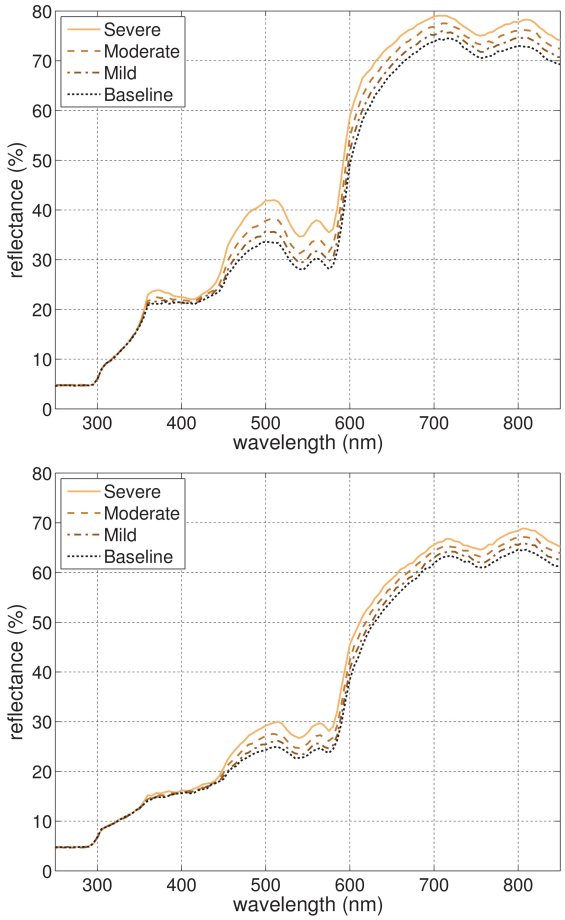

Figure 3.4: Modeled skin reflectance curves for the palmar fingertips of the lightly (top) and the darkly (bottom) pigmented specimen sshowing the spectral responses elicited by distinct dermal Hb concentrations associated with increasing anemia severity levels, namely baseline (nonanemic level, 147.0 g/L), mild (117.6 g/L), moderate (88.2 g/L) and severe (58.8 g/L). The modeled curves were obtained considering the data provided in Tables 2.2, 2.3 and 2.4.

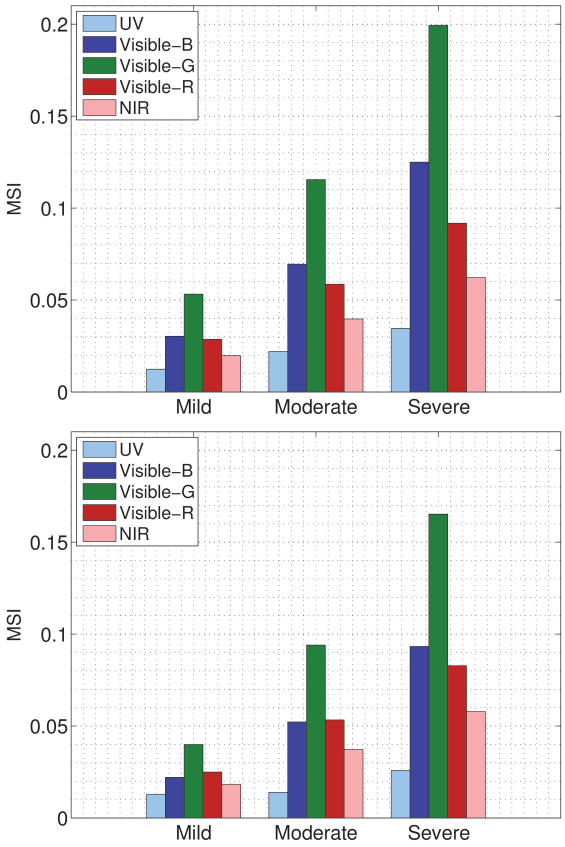

Figure 3.5: Mean sensitivity index (MSI) values computed for the modeled anemic skin reflectance curves (mild, moderate and severe) obtained for the palmar fingertips of the lightly (top) and the darkly (bottom) pigmented specimens (Figure 3.4). The MSI values were computed for each anemic skin reflectance curve (across selected UV (250-400 nm), Visible-B (400-500 nm), Visible-G (500-600 nm), Visible-R (600-700 nm), and NIR (700-850 nm) ranges) with respect to the baseline curve (nonanemic level) associated with the respective specimen.

Figure 3.6: Skin swatches depicting skin tone variations on the palmar fingertips of the lightly (top) and the darkly (bottom) pigmented specimens. These variations, which were obtained by reducing the dermal Hb concentration (from left to right, 147.0 g/L, 117.6 g/L, 88.2 g/L and 58.8 g/L), illustrate the visual effects of increasing anemia severity levels, namely baseline (nonanemic level), mild, moderate and severe, respectively (Table 2.4). The swatches were rendered considering a D50 illuminant (Figure 2.4) and using the corresponding skin spectral responses provided by the HyLIoS model (Figure 3.4).

Chapter 4

Monitoring Procedure

The difficulties imposed by different levels of pigmentation on the visual inspection of skin specimens can be exacerbated by other factors such as the intensity and spectral power distribution of the light sources employed during their screening. For example, as illustrated in the palmar fingertip swatches of the LP specimen presented in Figure 4.1, an anemic-like appearance can be elicited by different combinations of these factors. More precisely, although the spectral response used in the generation of these swatches corresponds to the nonanemic (baseline) case, some of them have appearance attributes similar to those of the swatches associated with different anemia severity levels presented in Figure 3.6, which may lead to misinterpretations of an

Figure 4.1: Skin swatches illustrating skin tone variations on the fingertip of the lightly pigmented specimen (with a baseline Hb concentration equal to 147.0 g/L) resulting from employing distinct light sources (Figure 2.4), namely D65 (top row), D50 (middle row) and A (bottom row), whose default intensity value (left column) was increased by 15% (middle column) and 30% (right column). The swatches were rendered using skin spectral responses provided by the HyLIoS model [16], which, in turn, were obtained using the data provided in Tables 2.2 and 2.3.

individual's actual health status. The possibility of occurrence of such situations, which are usually associated with metamerism problems [34, 33], can also be verified when we compare some of the "nonanemic" swatches of the DP specimen presented in Figure 4.2 with the "anemic" swatches presented in Figure 3.6 for this specimen.

Several symptoms (*e.g.*, tiredness and faintness) and signs (*e.g.*, pale or yellowish skin mentioned earlier) provide clues to physicians about the possible onset of anemia in a patient [69]. In order to verify this possibility and deliver a diagnosis with a higher degree of certainty, physicians usually re-

Figure 4.2: Skin swatches illustrating skin tone variations on the fingertip of the darkly pigmented specimen (with a baseline Hb concentration equal to 147.0 g/L) resulting from employing distinct light sources (Figure 2.4), namely D65 (top row), D50 (middle row) and A (bottom row), whose default intensity value (left column) was increased by 15% (middle column) and 30% (right column). The swatches were rendered using skin spectral responses provided by the HyLIoS model [16], which, in turn, were obtained using the data provided in Tables 2.2 and 2.3.

quire a blood exam. This is used to determine, among other factors, whether or not the patient's Hb concentration is below the level considered normal for people within the same age group and with similar physiological characteristics. Once it has been established that the patient is anemic and the recommended treatment starts, the condition should be monitored to evaluate whether or not the patient's Hb concentration is returning to the normal level. Again, clinical assessment procedures, such as visual inspections and blood exams can be employed [69]. We remark, however, that while the former may lead to incorrect interpretations as illustrated before, the latter

may be not readily available at the point of care on a regular basis.

The results of our second set of *in silico* experiments suggest that the monitoring of anemia can be assisted by an index, henceforth referred to AMI (Anemia Monitoring Index), which can be obtained through a noninvasive spectrophometric measurement performed at the patient's palmar fingertip. As depicted in Figures 3.4 and 3.5, variations on Hb concentration have a detectable impact on the palmar fingertip reflectance of specimens with distinct levels of native skin pigmentation, more prominently in the visible-G spectral region. Moreover, this impact is uniform in this region, *i.e.*, as the Hb concentration decreases, the reflectance increases across the entire 500-600 nm range. This suggests that a single sample wavelength within this range can be used to monitor these variations. Considering that the monitoring of an anemic patient may need to take place within an extended period of time, it is necessary to mitigate the chances of its results being affected by other physiologic factors.

In order to address this issue, a number of guidelines should be used in the selection of a suitable monitoring point. First, it should be a wavelength at which O_2Hb and HHb have the same extinction coefficient values (isosbestic point [84]) to avoid influences from changes in the blood oxygenation levels.

We note that there are several isosbestic points (500, 530, 545, 570 and 584 nm [32]) in the spectral region of interest (Figure 2.2). Second, it should be located away from the spectral region where water and lipids have a strong impact on light absorption [4, 16] to avoid masking effects, for example, from transepidermal water loss [12]. Third, it should be also located away from the absorption spectra of other chromophores associated with the onset of medical conditions with similar effects on a patient's visual appearance attributes. As a characteristic example of the latter, one can mention bilirubin [58], whose excess in the blood stream is associated with hyperbilirubinemia, or jaundice, which can also result in possible variations on skin appearance attributes (*e.g.*, yellowness) of a patient. Taking these guidelines into consideration, two isosbestic wavelengths, namely 545 and 570 nm, emerge as the most suitable candidates for being the monitoring point. It is also necessary to consider that even though the presence of melanin proteins in the palmar fingertip epidermis is fairly low, it cannot be completely discarded [78]. Hence, since the corresponding extinction coefficient values for the melanins are lower at the 570 nm than at 545 nm (Figure 2.2), we selected the former.

A relatively simple anemia monitoring procedure could be then employed using a single reflectance measurement at 570 nm. Preferably, the patient's

finger should be in a position below heart level to maximize the blood fractional volume [68], with the patient's forearm resting passively to minimize shear rate fluctuations on the blood flow that could affect its optical properties [80]. Moreover, since this measurement might need to be repeated a number of times during the treatment, it would be advisable to select a specific measurement site (*e.g.*, at the center of the tactile elevations) for consistency. Although the adoption of this protocol would contribute to make the procedure more effective, one may still need to account for the possibility of small changes in the measurement conditions. For example, one can expect small angular variations with respect to the angle of incidence due to slight curvature of the palmar fingertip. In order to examine the robustness of the proposed procedure with respect to such fluctuations, we computed the reflectance at 570 nm for the LP and DP specimens considering three angles of incidence, namely 0°, 10° (the default value employed in our *in silico* experiments) and 20°. Furthermore, since the anemia severity levels may vary with age and, in the case of female patients, pregnancy [77], we performed these computations with respect to a broader scope of Hb concentrations by including all values depicted in Tables 2.4 and 2.5.

As expected, the resulting reflectance values presented in Table 4.1 for

all three angles of incidence depict a "vertical" increase with respect to Hb concentration reduction, which becomes more prominent as the condition worsens. Moreover, for each specific Hb concentration value, they also show a slight "horizontal" increase with respect to the angle of incidence. In some instances, however, the same value was recorded for two angles of incidence. This can be attributed to the stochastic nature of our simulations. More importantly, the observed "horizontal" reflectance variations with the angle of incidence are smaller than the "vertical" reflectance variations associated with significant changes in the Hb concentration.

It is worth noting that even well designed and carefully calibrated spectrophotometers can yield results from the same specimen that differ from one measurement to the next [38, 7]. These differences, or uncertainties, are caused by variations in the components of the instrument, fluctuations in environmental conditions and changes in the specimen handling procedure. A spectrophotometer is considered to be of high precision if the spectral measurements have an uncertainty of approximately ± 0.001 [38, 46]. Hence, the "horizontal" reflectance variations depicted in our simulations have a magnitude comparable to the uncertainty of actual spectral measurements.

	LP			DP		
Hb Concentration (g/L)	$0°$	$10°$	$20°$	$0°$	$10°$	$20°$
147.0	0.290	0.290	0.289	0.241	0.241	0.240
125.0	0.301	0.301	0.300	0.248	0.247	0.246
117.6	0.306	0.306	0.303	0.251	0.251	0.249
100.0	0.318	0.317	0.316	0.258	0.258	0.258
88.2	0.329	0.328	0.327	0.266	0.265	0.264
75.0	0.342	0.342	0.341	0.275	0.273	0.273
58.8	0.365	0.364	0.364	0.289	0.288	0.288
50.0	0.381	0.381	0.379	0.301	0.300	0.298

Table 4.1: Reflectance values at 570 nm computed for the palmar fingertip of the lightly pigmented (LP) and the darkly pigmented (DP) specimens considering distinct hemoglobin (Hb) concentrations and three angles of incidence, namely $0°$, $10°$ (the default value used in this investigation) and $20°$. Each reflectance value was computed using 10^6 sample rays and depicted using a four-digit chopping arithmetic.

In summary, our findings suggest that once the onset of anemia has been established, this blood disorder can be reliably monitored using a relative simple procedure. At the time of the onset confirmation, the patient's AMI would measured and recorded. Afterwords, during the treatment, the patient's anemic level could be monitored by performing subsequent AMI measurements, and comparing their values with previously recorded ones. Clearly, a more accurate assessment can be obtained through blood exams performed using traditional laboratory procedures. However, considering that the proposed AMI would be obtained through a reflectance measurement performed at single wavelength, we believe that it would require a simpler and more cost-effective device than a standard spectrophotometer, making its use attractive for low-resources diagnosis settings with limited access to laboratory facilities. We also remark that such a measurement would be noninvasive and performed at a wavelength within the visible (non-harmful) region of the light spectrum.

Chapter 5

Conclusion

Arguably anemia is among the most widespread of blood disorders that can lead to serious health impairment and, if not properly treated, fatal situations. Not surprisingly, the physiological changes associated with this condition, particularly the reduction of Hb concentration, have been object of extensive research aimed at their quantification and interpretation. The biomedical procedures employed in these tasks vary from a simple visual inspection of a patient's appearance to a wide range of laboratory exams of blood samples. With the recent advances in optics and photonics, a wide range of invasive and noninvasive devices are being proposed to assist these tasks. In the later case, the reliability of the results depends on the correct

assessment of the skin spectral responses to these changes. However, the *in vivo* investigation of these responses is often hindered by practical difficulties such as the the control of a large number of biophysical variables.

In this thesis, we employed a first principles light transport model of light and skin interactions to examine these responses with respect to different spectral, observational and physiological conditions. The results of our controlled *in silico* experiments demonstrate that the influence of melanin pigmentation on the effective detection of these responses can be substantially mitigated by selecting a cutaneous site, such as the palmar fingertip, with suitable characteristics, namely hypopigmentation and increased dermal blood content. Furthermore, our findings also indicate that significant variations in the anemia severity levels associated with Hb concentration reductions can be monitored by measuring the patient's skin reflectance at a selected spectral sampling point (570 nm) neither affected by blood oxygenation variations nor by changes in the presence of other relevant absorbers (*e.g.*, bilirubin and water) in the skin tissues. Based on these observations, we proposed the use of such reflectance (AMI) measurements as the integral component of a procedure to assist the monitoring of anemic patients in regions not served by comprehensive health care resources on a regular basis.

As future work, we intend to address the actual implementation of the proposed anemia monitoring procedure. Accordingly, we plan to investigate the feasibility of different alternatives for performing the AMI measurements at the point-of-care. These include the enhancement of existing devices to incorporate AMI measurements, and the design of a new portable instrument specifically dedicated to providing this index with a high accuracy to cost ratio.

Bibliography

[1] P. Agache. Main skin biological constants. In P. Agache and P. Humbert, editors, *Measuring the Skin*, pages 727–746. Springer-Berlag, Berlin, Germany, 2004.

[2] S. Alaluf, D. Atkins, K. Barret, M. Blount, N. Carter, and A. Heath. Ethnic variation in melanin content and composition in photoexposed and photoprotected human skin. *Pigment Cell Research*, 15:112–118, 2002.

[3] R.R. Anderson and J.A. Parrish. The optics of human skin. *Invest Dermatol*, 77(1):13–9, 1981.

[4] R.R. Anderson and J.A. Parrish. Optical properties of human skin. In J.D. Regan and J.A. Parrish, editors, *The Science of Photomedicine*, pages 147–194, N.Y., USA, 1982. Plenun Press.

[5] E. Angelopoulou. Understanding the color of human skin. In *Storage and Retrieval for Image and Video Databases*, 2001.

[6] G. V. G. Baranoski, T. F. Chen, B. W. Kimmel, E. Miranda, and D. Yim. On the noninvasive optical monitoring and differentiation of methemoglobinemia and sulfhemoglobinemia. *Journal of Biomedical Optics*, 17(9):097005–1–14, 2012.

[7] G. V. G. Baranoski and A. Krishnaswamy. *Light & Skin Interactions: Simulations for Computer Graphics Applications*. Morgan Kaufmann/Elsevier, Burlington, MA, USA, 2010.

[8] G.V.G. Baranoski, T.F. Chen, and A. Krishnaswamy. Multilayer modeling of skin color and translucency. In B. Querleux, editor, *Computational Biosphysics of the Skin*, pages 3–24. Pan Stanford Publishing, Singapore, 2014.

[9] G.V.G. Baranoski, T. Dimson, T. F. Chen, B. Kimmel, D. Yim, and E. Miranda. Rapid dissemination of light transport models on the web. *IEEE Computer Graphics and Applications*, 32:10–15, 2012.

[10] G.V.G. Baranoski, J.G. Rokne, and G. Xu. Virtual spectrophotometric measurements for biologically and physically-based rendering. *The Visual Computer*, 17(8):506–518, 2001.

[11] A. N. Bashkatov, E. A. Genina, V. I. Kochubey, M. M. Stolnitz, T. A. Bashkatova, O. V. Novikova, A. Y. Peshkova, and V. V. Tuchin. Optical properties of melanin in the skin and skin-like phantoms. In Valery V. Tuchin, editor, *Controlling Tissue Optical Properties: Applications in Clinical Study*, volume 4162, pages 219–226. SPIE, 2000.

[12] I. Blank. Factors which influence the water content of the stratum corneum. *J. Investig. Dermatol.*, 18(6):433–440, 06 1952.

[13] M. Bond, C. Elguea, J.S. Yan, M. Pawlowski, J. Williams, A. Wahed amd M. Oden, T.S. Tkaczyk, and R. Richards-Kortum. Chromatography paper as a low-cost medium for accurate spectrophotometric assessment of blood hemoglobin concentration. *Lab Chip*, 13:2381–2388, 2013.

[14] M. Bond, J. Mvula, E. Molyneux, and R. Richards-Kortum. Design and performance of a low-cost, handheld reader for diagnosing anemia in

Blantyre, Malawi. In *Health Innovations and Point-of-Care Technologies Conference*, pages 267–270, Seattle, Washington, USA, October 2014.

[15] A. E. Cerussi, A. J. Berger, F. Bevilacqua, N. Shah, D. Jakubowski, J. Butler, R. F. Holcombe, and B. J. Tromberg. Sources of absorption and scattering contrast for near-infrared optical mammography. *Academic radiology*, 8(3):211–218, March 2001.

[16] T.F. Chen, G.V.G. Baranoski, B.W. Kimmel, and E. Miranda. Hyperspectral modeling of skin appearance. *ACM Transactions on Graphics*, 34(3):31:1–14, 2015.

[17] C. Crowley, G. Montenegro-Bethancourt, N.W. Solomons, and K. Schumann. Validity and correspondence of non-invasively determined hemoglobin concentrations by two trans-cutaneous digital measuring devices. *Asia Pacific Journal of Clinical Nutrition*, 21(2):191–200, January 2012.

[18] W. Cui, L.E. Ostrander, and B.Y. Lee. *In Vivo* reflectance of blood and tissue as a function of light wavelength. *IEEE Transactions on Biomedical Engineering*, 37(6):632–639, 1990.

We note that there are several isosbestic points (500, 530, 545, 570 and 584 nm [32]) in the spectral region of interest (Figure 2.2). Second, it should be located away from the spectral region where water and lipids have a strong impact on light absorption [4, 16] to avoid masking effects, for example, from transepidermal water loss [12]. Third, it should be also located away from the absorption spectra of other chromophores associated with the onset of medical conditions with similar effects on a patient's visual appearance attributes. As a characteristic example of the latter, one can mention bilirubin [58], whose excess in the blood stream is associated with hyperbilirubinemia, or jaundice, which can also result in possible variations on skin appearance attributes (*e.g.*, yellowness) of a patient. Taking these guidelines into consideration, two isosbestic wavelengths, namely 545 and 570 nm, emerge as the most suitable candidates for being the monitoring point. It is also necessary to consider that even though the presence of melanin proteins in the palmar fingertip epidermis is fairly low, it cannot be completely discarded [78]. Hence, since the corresponding extinction coefficient values for the melanins are lower at the 570 nm than at 545 nm (Figure 2.2), we selected the former.

A relatively simple anemia monitoring procedure could be then employed using a single reflectance measurement at 570 nm. Preferably, the patient's

finger should be in a position below heart level to maximize the blood fractional volume [68], with the patient's forearm resting passively to minimize shear rate fluctuations on the blood flow that could affect its optical properties [80]. Moreover, since this measurement might need to be repeated a number of times during the treatment, it would be advisable to select a specific measurement site (*e.g.*, at the center of the tactile elevations) for consistency. Although the adoption of this protocol would contribute to make the procedure more effective, one may still need to account for the possibility of small changes in the measurement conditions. For example, one can expect small angular variations with respect to the angle of incidence due to slight curvature of the palmar fingertip. In order to examine the robustness of the proposed procedure with respect to such fluctuations, we computed the reflectance at 570 nm for the LP and DP specimens considering three angles of incidence, namely 0°, 10° (the default value employed in our *in silico* experiments) and 20°. Furthermore, since the anemia severity levels may vary with age and, in the case of female patients, pregnancy [77], we performed these computations with respect to a broader scope of Hb concentrations by including all values depicted in Tables 2.4 and 2.5.

As expected, the resulting reflectance values presented in Table 4.1 for

all three angles of incidence depict a "vertical" increase with respect to Hb concentration reduction, which becomes more prominent as the condition worsens. Moreover, for each specific Hb concentration value, they also show a slight "horizontal" increase with respect to the angle of incidence. In some instances, however, the same value was recorded for two angles of incidence. This can be attributed to the stochastic nature of our simulations. More importantly, the observed "horizontal" reflectance variations with the angle of incidence are smaller than the "vertical" reflectance variations associated with significant changes in the Hb concentration.

It is worth noting that even well designed and carefully calibrated spectrophotometers can yield results from the same specimen that differ from one measurement to the next [38, 7]. These differences, or uncertainties, are caused by variations in the components of the instrument, fluctuations in environmental conditions and changes in the specimen handling procedure. A spectrophotometer is considered to be of high precision if the spectral measurements have an uncertainty of approximately ± 0.001 [38, 46]. Hence, the "horizontal" reflectance variations depicted in our simulations have a magnitude comparable to the uncertainty of actual spectral measurements.

	LP			DP		
Hb Concentration (g/L)	$0°$	$10°$	$20°$	$0°$	$10°$	$20°$
147.0	0.290	0.290	0.289	0.241	0.241	0.240
125.0	0.301	0.301	0.300	0.248	0.247	0.246
117.6	0.306	0.306	0.303	0.251	0.251	0.249
100.0	0.318	0.317	0.316	0.258	0.258	0.258
88.2	0.329	0.328	0.327	0.266	0.265	0.264
75.0	0.342	0.342	0.341	0.275	0.273	0.273
58.8	0.365	0.364	0.364	0.289	0.288	0.288
50.0	0.381	0.381	0.379	0.301	0.300	0.298

Table 4.1: Reflectance values at 570 nm computed for the palmar fingertip of the lightly pigmented (LP) and the darkly pigmented (DP) specimens considering distinct hemoglobin (Hb) concentrations and three angles of incidence, namely $0°$, $10°$ (the default value used in this investigation) and $20°$. Each reflectance value was computed using 10^6 sample rays and depicted using a four-digit chopping arithmetic.

In summary, our findings suggest that once the onset of anemia has been established, this blood disorder can be reliably monitored using a relative simple procedure. At the time of the onset confirmation, the patient's AMI would measured and recorded. Afterwords, during the treatment, the patient's anemic level could be monitored by performing subsequent AMI measurements, and comparing their values with previously recorded ones. Clearly, a more accurate assessment can be obtained through blood exams performed using traditional laboratory procedures. However, considering that the proposed AMI would be obtained through a reflectance measurement performed at single wavelength, we believe that it would require a simpler and more cost-effective device than a standard spectrophotometer, making its use attractive for low-resources diagnosis settings with limited access to laboratory facilities. We also remark that such a measurement would be noninvasive and performed at a wavelength within the visible (non-harmful) region of the light spectrum.

Chapter 5

Conclusion

Arguably anemia is among the most widespread of blood disorders that can lead to serious health impairment and, if not properly treated, fatal situations. Not surprisingly, the physiological changes associated with this condition, particularly the reduction of Hb concentration, have been object of extensive research aimed at their quantification and interpretation. The biomedical procedures employed in these tasks vary from a simple visual inspection of a patient's appearance to a wide range of laboratory exams of blood samples. With the recent advances in optics and photonics, a wide range of invasive and noninvasive devices are being proposed to assist these tasks. In the later case, the reliability of the results depends on the correct

assessment of the skin spectral responses to these changes. However, the *in vivo* investigation of these responses is often hindered by practical difficulties such as the the control of a large number of biophysical variables.

In this thesis, we employed a first principles light transport model of light and skin interactions to examine these responses with respect to different spectral, observational and physiological conditions. The results of our controlled *in silico* experiments demonstrate that the influence of melanin pigmentation on the effective detection of these responses can be substantially mitigated by selecting a cutaneous site, such as the palmar fingertip, with suitable characteristics, namely hypopigmentation and increased dermal blood content. Furthermore, our findings also indicate that significant variations in the anemia severity levels associated with Hb concentration reductions can be monitored by measuring the patient's skin reflectance at a selected spectral sampling point (570 nm) neither affected by blood oxygenation variations nor by changes in the presence of other relevant absorbers (*e.g.*, bilirubin and water) in the skin tissues. Based on these observations, we proposed the use of such reflectance (AMI) measurements as the integral component of a procedure to assist the monitoring of anemic patients in regions not served by comprehensive health care resources on a regular basis.

As future work, we intend to address the actual implementation of the proposed anemia monitoring procedure. Accordingly, we plan to investigate the feasibility of different alternatives for performing the AMI measurements at the point-of-care. These include the enhancement of existing devices to incorporate AMI measurements, and the design of a new portable instrument specifically dedicated to providing this index with a high accuracy to cost ratio.

Bibliography

[1] P. Agache. Main skin biological constants. In P. Agache and P. Humbert, editors, *Measuring the Skin*, pages 727–746. Springer-Berlag, Berlin, Germany, 2004.

[2] S. Alaluf, D. Atkins, K. Barret, M. Blount, N. Carter, and A. Heath. Ethnic variation in melanin content and composition in photoexposed and photoprotected human skin. *Pigment Cell Research*, 15:112–118, 2002.

[3] R.R. Anderson and J.A. Parrish. The optics of human skin. *Invest Dermatol*, 77(1):13–9, 1981.

[4] R.R. Anderson and J.A. Parrish. Optical properties of human skin. In J.D. Regan and J.A. Parrish, editors, *The Science of Photomedicine*, pages 147–194, N.Y., USA, 1982. Plenun Press.

[5] E. Angelopoulou. Understanding the color of human skin. In *Storage and Retrieval for Image and Video Databases*, 2001.

[6] G. V. G. Baranoski, T. F. Chen, B. W. Kimmel, E. Miranda, and D. Yim. On the noninvasive optical monitoring and differentiation of methemoglobinemia and sulfhemoglobinemia. *Journal of Biomedical Optics*, 17(9):097005–1–14, 2012.

[7] G. V. G. Baranoski and A. Krishnaswamy. *Light & Skin Interactions: Simulations for Computer Graphics Applications*. Morgan Kaufmann/Elsevier, Burlington, MA, USA, 2010.

[8] G.V.G. Baranoski, T.F. Chen, and A. Krishnaswamy. Multilayer modeling of skin color and translucency. In B. Querleux, editor, *Computational Biosphysics of the Skin*, pages 3–24. Pan Stanford Publishing, Singapore, 2014.

[9] G.V.G. Baranoski, T. Dimson, T. F. Chen, B. Kimmel, D. Yim, and E. Miranda. Rapid dissemination of light transport models on the web. *IEEE Computer Graphics and Applications*, 32:10–15, 2012.

[10] G.V.G. Baranoski, J.G. Rokne, and G. Xu. Virtual spectrophotometric measurements for biologically and physically-based rendering. *The Visual Computer*, 17(8):506–518, 2001.

[11] A. N. Bashkatov, E. A. Genina, V. I. Kochubey, M. M. Stolnitz, T. A. Bashkatova, O. V. Novikova, A. Y. Peshkova, and V. V. Tuchin. Optical properties of melanin in the skin and skin-like phantoms. In Valery V. Tuchin, editor, *Controlling Tissue Optical Properties: Applications in Clinical Study*, volume 4162, pages 219–226. SPIE, 2000.

[12] I. Blank. Factors which influence the water content of the stratum corneum. *J. Investig. Dermatol.*, 18(6):433–440, 06 1952.

[13] M. Bond, C. Elguea, J.S. Yan, M. Pawlowski, J. Williams, A. Wahed amd M. Oden, T.S. Tkaczyk, and R. Richards-Kortum. Chromatography paper as a low-cost medium for accurate spectrophotometric assessment of blood hemoglobin concentration. *Lab Chip*, 13:2381–2388, 2013.

[14] M. Bond, J. Mvula, E. Molyneux, and R. Richards-Kortum. Design and performance of a low-cost, handheld reader for diagnosing anemia in

Blantyre, Malawi. In *Health Innovations and Point-of-Care Technologies Conference*, pages 267–270, Seattle, Washington, USA, October 2014.

[15] A. E. Cerussi, A. J. Berger, F. Bevilacqua, N. Shah, D. Jakubowski, J. Butler, R. F. Holcombe, and B. J. Tromberg. Sources of absorption and scattering contrast for near-infrared optical mammography. *Academic radiology*, 8(3):211–218, March 2001.

[16] T.F. Chen, G.V.G. Baranoski, B.W. Kimmel, and E. Miranda. Hyperspectral modeling of skin appearance. *ACM Transactions on Graphics*, 34(3):31:1–14, 2015.

[17] C. Crowley, G. Montenegro-Bethancourt, N.W. Solomons, and K. Schumann. Validity and correspondence of non-invasively determined hemoglobin concentrations by two trans-cutaneous digital measuring devices. *Asia Pacific Journal of Clinical Nutrition*, 21(2):191–200, January 2012.

[18] W. Cui, L.E. Ostrander, and B.Y. Lee. *In Vivo* reflectance of blood and tissue as a function of light wavelength. *IEEE Transactions on Biomedical Engineering*, 37(6):632–639, 1990.

[19] A. J. Cunnington, S. F. W. Kendrick, B. Wamola, B. Lowe, and C. R. J. C. Newton. Carboxyhemoglobin levels in kenyan children with plasmodium falciparum malaria. *The American Journal of Tropical Medicine and Hygiene*, 71(1):43–47, 2004.

[20] B. de Benoist, E. McLean, I. Egli, and M. Cogswell, editors. *Worldwide prevalence of anaemia 1993-2005 WHO Global Database on Anaemia*, Geneva, Switzerland, 2008. World Health Organization.

[21] B. L. Diffey. Ultraviolet radiation physics and the skin. *Physics in Medicine and Biology*, 25(3):405, 1980.

[22] B.L. Diffey. A mathematical model for ultraviolet optics in skin. *Physics in Medicine and Biology*, 28(6):647–657, 1983.

[23] R. Doshi and A. Panditrao. Non-invasive Optical Sensor for Hemoglobin Determination. *International Journal of Engineering Research and Applications*, 3(2):559–562, March-April 2013.

[24] R. Flewelling. Noninvasive optical monitoring. In Joseph D. Bronzino, editor, *The Biomedical Engineering Handbook*. CRC Press LLC, 2 edition, 2000.

[25] R. Flindt. *Amazing Numbers in Biology.* Springer-Verlag, Berlin, Germany, 2006.

[26] E. Fuchs. Keratins and the skin. *Annual Review of Cell and Developmental Biology*, 11(1):123–154, 1995.

[27] D. J. Gawkrodger and M.R. Ardern-Jones. *Dermatology An Illustrated Colour Text.* Churchill Livingstone, Elsevier, 3rd edition, 2002.

[28] D.M. Hamby. A review of techniques for parameter sensitivity analysis of environmental models. *Environ. Monit. Assess.*, 32:135–154, 1994.

[29] A. Hennessy, C. Oh, B. Diffey, K. Wakamatsu, S. Ito, and J. Rees. Eumelanin and pheomelanin concentrations in human epidermis before and after UVB irradiation. *Pigment Cell Research*, 18:220–223, 2005.

[30] J.J. Hopfield. Olfation and color vision: more in simpler. In N.P. Ong and R.N. Bhatt, editors, *More is Different: Fifty Years of Condensed Matter Physics*, pages 269–284, Princeton, NJ. USA, 2001. Princeton University Press.

[31] S. Hu and L. V. Wang. Photoacoustic imaging and characterization of microvasculature. *Journal of Biomedical Optics*, 15(1):011101:1–15, 2010.

[32] R. W. G. Hunt. *Measuring Colour*. Ellis Horwood Limited, Chichester, England, 2nd edition, 1991.

[33] R.S. Hunter and R.W. Harold. *The Measurement of Appearance*. John Wiley & Sons, New York, NY, USA, second edition, 1987.

[34] S. L. Jacques. Origins of tissue optical properties in the UVA, visible, and NIR regions. *OSA TOPS on Adv. in Opt. Imaging and Photon Migration*, 2:364–369, 1996.

[35] S. L. Jacques. Optical absorption of melanin. Technical report, Oregon Medical Laser Center, 2001.

[36] S. L. Jacques, C. A. Alter, and S. A. Prahl. Angular dependence of HeNe laser light scattering by human dermis. *Lasers Life Sci.*, 1:309–333, 1987.

[37] D.B. Judd and G. Wyszecki. *Color in Business, Science and Industry*. John Wiley & Sons, New York, NY, USA, third edition, 1975.

[38] N. Kollias, R. M. Sayre, L. Zeise, and M. R. Chedekel. Photoprotection by melanin. *J. Photoch. Photobio. B.*, 9(2):135–60, 1991.

[39] J. Kraitl, D. Klinger, D. Fricke, U. Timm, and H. Ewald. Non-invasice measurement of blood components. Sensors for an in-vivo hemoglobin measurement. *Advancement in Sensing Technology, Smart Sensors, Measurement and Instrumentation*, 1:237–262, 2013.

[40] A. Krishnaswamy, G.V.G. Baranoski, and Jon G. Rokne. Improving the reliability/cost ratio of goniophotometric measurements. *Journal of Graphics Tools*, 9(3):31–51, 2004.

[41] L. Lamhaut, R. Apriotesei, X. Combes, M. Lejay, P. Carli, and B. Vivien. Comparison of the accuracy of noninvasive hemoglobin monitoring by spectrophotometry (SpHb) and HemoCue with automated laboratory hemoglobin measurement. *Anesthesiology*, 115(3):548–554, 2011.

[42] R. Lee, M. M. Mathews-Roth, M. A. Pathak, and J. A. Parrish. The detection of carotenoid pigments in human skin. *J Investig Dermatol*, 64(3):175–177, 1975.

[43] T. S. Lister. *Simulating the Color of Port Wine Stain Skin*. PhD thesis, University of Southampton,U.K., February 2013.

[44] A. T. Lovell, J. C. Hebden, J. C. Goldstone, and M. Cope. Determination of the transport scattering coefficient of red blood cells. In *Proc. SPIE 3597, Optical Tomography and Spectroscopy of Tissue III*, volume 3597, pages 175–182, 1999.

[45] D.L. MacAdam. *Color Measurements Theme and Variations*. Springer Verlag, Berlin, Germany, 1981.

[46] N. Magnenat-Thalmann, P. Kalra, J. L. Leveque, R. Bazin, D. Batisse, and B. Querleux. A computational skin model: fold and wrinkle formation. *Information Technology in Biomedicine, IEEE Transactions on*, 6(4):317–323, 2002.

[47] A. Maton, J. Hopkins, C. W. McLaughlin, S. Johnson, M. Q. Warner, D. LaHart, and J.D. Wright. *Human Biology and Health*. Prentice Hall, Englewood Cliffs, N.J., USA, 1993.

[48] E. McLean, M. Cogswell, I. Egli, D. W. Wojdyla, and B. de Benoist. Worldwide prevalence of anaemia, WHO Vitamin and Mineral Nutrion System, 1993-2005. *Public Health Nutrition*, 12(3):444–454, 2003.

[49] I. Meglinski, A. Doronin, A .N. Bashkatov, E. A. Genina, and V. V. Tuchin. Dermal component-based optical modeling of skin translucency: Impact on skin color. In B. Querleux, editor, *Computational Biosphysics of the Skin*, pages 25–62. Pan Stanford Publishing, Singapore, 2014.

[50] N. Nakagawa, M. Matsumoto, and S. Sakai. *In vivo* measurement of the water content in the dermis by confocal Raman spectroscopy. *Skin Research and Technology*, 16(2):137–141, 2010.

[51] Natural Phenomena Simulation Group (NPSG). *Run HyLIoS Online*. School of Computer Science, University of Waterloo, Ontario, Canada, 2014. http://www.npsg.uwaterloo.ca/models/hylios.php.

[52] K. P. Nielsen, L. Zhao, J. J. Stamnes, K. Stamnes, and J. Moan. The importance of the depth distribution of melanin in skin for DNA protection and other photobiological processes. *J. Photoch. Photobio. B.*, 82(3):194–198, 2006.

[53] N. Ohta and A.R. Robertson. *Colorimetry Fundamentals and Applications*. John Wiley & Sons, New York, NY, USA, 1982.

[54] R. L. Olson, J. Gaylor, and M. A. Everett. Skin color, melanin, and erythema. *Arch. Dermatol.*, 108(4):541–544, 1973.

[55] M.A. Pathak. Functions of melanin and protection by melanin. In M.R. Chedekel L. Zeise and T.B. Fitzpatrick, editors, *Melanin: Its Role in Human Photoprotection*, pages 125–134, Overland Park, Kansas, USA, 1995. Valdenmar Publishing Co.

[56] S. A. Prahl. Optical absorption of hemoglobin. Technical report, Oregon Medical Laser Center, 1999.

[57] S. A. Prahl. PhotochemCAD spectra by category. Technical report, Oregon Medical Laser Center, 2001.

[58] C.S. Eby S. Haymond, R. Cariappa and M.G. Scott. Laboratory assessment of oxygenation in methemoglobinemia. *Clinical Chemistry*, 51(2):434–444, 2005.

[59] H. Schenck, M. Falkensson, and B. Lundberg. Evaluation of "HemoCue", a new device for determing hemoglobin. *Clinical Chemistry*, 32(3):526–529, 1986.

[60] H. Shimizu. *Shimizu's Textbook of Dermatology*. Hokkaido University Press, 2007.

[61] C. A. Squier, P. Cox, and P. W. Wertz. Lipid content and water permeability of skin and oral mucosa. *Journal of Investigative Dermatology*, 96(1):123–126, 1991.

[62] M.C. Stone. *A Field Guide to Digital Color*. AK Peters, Natick, MA, USA, 2003.

[63] P. S. Talreja, G. B. Kasting, N. K. Kleene, W. L. Pickens, and T. Wang. Visualization of the lipid barrier and measurement of lipid pathlength in human stratum corneum. *AAPS PharmSci*, 3(2):48–56, 2001.

[64] G. J. Tearney, M. E. Brezinski, J. F. Southern, B. E. Bouma, M. R. Hee, and J. G. Fujimoto. Determination of the refractive index of highly scattering human tissue by optical coherence tomography. *Opt. Lett.*, 20(21):2258–2260, Nov 1995.

[65] A. J. Thody, E. M. Higgins, K. Wakamatsu, S. Ito, S. A Burchill, and J. M. Marks. Pheomelanin as well as eumelanin is present in human epidermis. *J Investig Dermatol*, 97(2):340–344, 08 1991.

[66] V.V. Tuchin. *Tissue optics: light scattering methods and instruments for medical diagnosis*. SPIE PM. SPIE/International Society for Optical Engineering, Bellingham, WA, USA, 2007.

[67] R.H. Turner, G.E. Burch, and W.A. Sodeman. Studies in the physiology of blood vessels in man. III. Some effects of raising and lowering the arm upon the pulse volume and blood volume of the human finger tip in health and in certain diseases of the blood vessels. *The Journal of Clinical Investigation*, 16(5):789–798, 1937.

[68] US Department of Health and Human Services. Your guide to anemia. Technical Report NIH 11-7629, National Institutes of Health, National Heart, Lung and Blood Institute, September 2011.

[69] J. S. Varcoe. *Clinical Biochemistry: Techniques and Instrumentation A Practical Course*. World Scientific, Singapore, 2001.

[70] B.D. Ventura, C. Lemerle, K. Michalodimitrakis, and L. Serrano. From *in vivo* to *in silico* biology and back. *Nature*, 443:527–553, 2006.

[71] J. A. Viator, J. Komadina, L. O. Svaasand, G. Aguilar, B. Choi, and N.J. Stuart. A comparative study of photoacoustic and reflectance methods for determination of epidermal melanin content. *Journal of Investigative Dermatology*, 122(6):1432–1439, 06 2004.

[72] L. Wang, S.L. Jacques, and L. Zheng. MCML – Monte Carlo modelling of light transport in multi-layered tissues. *Computer Methods and Programs in Biomedicine*, 47:131–146, 1995.

[73] S. Watanabe, S. Yamamoto, M. Yamauchi, N. Tsumura, K. Ogawa-Ochiai, and T. Akiba. Measuring hemoglobin amount and oxygen saturation of skin with advancing age. In Gerard L. Coté and Robert J. Nordstrom, editors, *Optical Diagnostics and Sensing XII: Toward Point-of-Care Diagnostics; and Design and Performance Validation of Phantoms Used in Conjunction with Optical Measurement of Tissue IV*, volume 8229. Society of Photo-Optical Instrumentation Engineers, February 2012.

[74] J.T. Whitton and J.D. Everall. The thickness of the epidermis. *British Journal of Dermatology*, 89:467–476, 1973.

[75] M. L Williams, M. Hincenbergs, and K. A. Holbrook. Skin lipid content during early fetal development. *Journal of Investigative Dermatology*, 91(3):263–268, 09 1988.

[76] World Health Organization. Haemoglobin concentrations for the diagnosis of anaemia and assessment of severity. In *VMNIS - Vitamin and*

Mineral Nutrition Information System, pages 1–6, Geneva, Switzerland, 2011. WHO/NMH/NHD/MnM/11.1.

[77] Y. Yamaguchi, S. Itami, H. Watabe, K. Yasumoto, Z. A. Abdel-Malek, T. Kubo, F. Rouzaud, A. Tanemura, K. Yoshikawa, and V.J. Hearing. Mesenchymal-epithelial interactions in the skin: increased expression of dickkopf1 by palmoplantar fibroblast inhibits melanocyte growth and differentiation. *Journal of Cell Biology*, 165(2):275–285, 2004.

[78] I. H. Yarynovska and A.I. Bilyi. Absorption spectra of sulfhemoglobin derivatives of human blood. In G.L. Cote and A.V. Priezzhev, editors, *Optical Diagnostics and Sensing VI*, volume 6094, pages 1–6. SPIE, 2006.

[79] D. Yim, G.V.G. Baranoski, B.W. Kimmel, T.F. Chen, and E. Miranda. A cell-based light interaction model for human blood. *Computer Graphics Forum*, 31(2):845–854, 2012.

[80] A. Yoshida, K. Saito, K. Ishi, I. Azuma, H. Sasa, and K. Furuya. Assessment of noninvasive, percutaneous hemoglobin measurement in pregnant and early postpartum women. *Medical Devices: Evidence and Research*, 7:11–16, January 2014.

[81] A. R. Young. Chromophores in human skin. *Physics in Medicine and Biology*, 42(5):789, 1997.

[82] P. Zakharov, M. S. Talary, and A. Caduff. A wearable diffuse reflectance sensor for continuous monitoring of cutaneous blood content. *Physics in Medicine and Biology*, 54(17), August 2009.

[83] H.F. Zhang, K. Maslov, and L.V. Wang. Dark-field confocal photoacoustic microscopy. In L. V. Wang, editor, *Photoaccoustic Imaging ans Spectroscopy*, number 822905, pages 267–280. CRC Press, February 2009.

[84] S.D. Zucker, P.S. Horn, and K.E. Sherman. Serum bilirubin levels in the US population: Gender effect and inverse correlation with colorectal cancer. *Hepatology*, 40(4):827–835, October 2004.

Index

Anemia, 2, 44

Anemia Monitoring Index, 38, 43

Anemia Severity, 19, 25

Anemia Symptoms, 12

Anemia Types, 12

Bilirubin, 12

Darkly Pigmented Specimen, 12

Gonioreflectometer, 12

Hemoglobin, 12

Hemolytic Anemia, 12

HyLIoS, 12

Invasive Devices, 12

Isosbestic Point, 12

Jaundice, 12

Keratin, 12

Lightly Pigmented Specimen, 12

Melanosomes, 12

Non-Invasive Devices, 12

Nonpalmoplantar Areas, 12

Palmar Areas, 12

Pernicious Anemia, 12

Pulse Oximetry, 12

Sensitivity Index, 12

Skin Swatches, 12

Spectrophotometer, 12

Spectrum, 12